

UniSteer: Text-Guided Flow Matching in Activation Space for Versatile LLM Steering

Yingdong Shi^{*}, Ruiming Zhang^{*}, Changming Li, Zhiyu Yang,
Kaixing Zhang, Jingyi Yu, Kan Ren[†]

ShanghaiTech University

{shiyd2023, zhangrm2022, renkan}@shanghaitech.edu.cn

^{*}Equal contribution. [†]Corresponding author.

Abstract

Activation-based control steers large language models (LLMs) by intervening on their internal representations during inference, and has emerged as an effective paradigm for controlling behaviors such as persona and style. However, existing methods often rely on fixed steering directions or task-specific intervention modules, making them difficult to adapt to fine-grained concepts and compositional constraints. We propose UNISTEER, a text-guided activation flow matching model that learns a conditional distribution over residual-stream activations from natural-language conditions. Instead of fitting a separate intervention for each target behavior, UNISTEER learns a universal conditional velocity field in activation space. At inference time, UNISTEER performs flow inversion by partially transporting a source activation toward a latent state and regenerating it under a target textual condition before injecting it back into the frozen LLM. The same conditional model supports activation-space classification by selecting the textual label with the lowest reconstruction energy. Experiments on three target LLMs show that UNISTEER provides a unified interface across behavioral control, truthfulness steering, fine-grained concept steering, multi-constraint instruction following, and activation-space classification.

1 Introduction

Controlling the behavior of large language models (LLMs) is central to their safe, reliable, and customizable deployment. One promising direction is activation-based control, which intervenes directly on the internal representations of a frozen LLM during inference (Turner et al., 2025; Panickssery et al., 2023; Li et al., 2023b; Zou et al., 2025). Compared with prompting or fine-tuning, activation intervention offers a lightweight and modular way to influence model behavior without updating model parameters, making it attractive for steering

properties such as truthfulness, refusal, persona, style, and instruction following.

Existing activation steering methods typically represent a target behavior as a fixed direction or task-specific intervention in activation space. Contrastive activation addition (Panickssery et al., 2023; Turner et al., 2025) estimates steering vectors from positive and negative examples, representation engineering (Zou et al., 2025) identifies behavior-relevant directions or subspaces, and learned intervention methods (Wu et al., 2024; Zhao et al., 2026; Luo et al., 2026) train modules to modify hidden states. Although effective in several settings, these approaches are often tied to predefined attributes, require separately fitted directions or modules for each target behavior, and struggle to compose multiple behavioral requirements because independently learned directions can interfere with one another in high-dimensional activation spaces.

We argue that activation steering can be more naturally formulated through *text-conditioned activation flow matching* (Lipman et al., 2023; Liu et al., 2022; Tong et al., 2023). Rather than constructing a separate intervention for each target behavior, the goal is to learn a conditional velocity field over LLM activations, where the editing dynamics are specified by a semantic text condition. This view provides a unified interface for heterogeneous control targets including behavioral traits, fine-grained concepts, and multi-constraint requirements. The control targets can all be expressed as textual conditions, while the same activation model defines the corresponding editing dynamics. In particular, compositional requirements can be represented directly in the condition text, avoiding post-hoc combinations of separately learned steering components.

In this work, we propose UNISTEER, a text-conditioned activation flow model for unified LLM steering and activation-space classification (Li et al., 2023a; Clark and Jaini, 2023). UNISTEER

learns a conditional velocity field over residual-stream activations of a frozen target LLM, where the condition is a natural-language description of the desired behavior, concept, or constraint. At inference time, UNISTEER edits an observed activation by partially inverting it under a source condition and then transporting it forward under a target condition. The same conditional activation model can also be used as an *activation-space classifier*. Given candidate textual labels, UNISTEER scores how well each condition explains an activation and predicts the label with the lowest conditional reconstruction energy.

Our contributions are threefold. First, we formulate activation steering as text-conditioned activation transport and introduce a conditional flow-matching model for LLM internal activations. Second, we propose flow inversion for inference-time activation editing, enabling a single model to handle behavioral traits, fine-grained concepts, and compositional constraints through natural-language conditions. Third, we show that the same conditional activation model can be used for activation-space classification via reconstruction energy.

2 Related Work

2.1 Representation Understanding

A growing body of work shows that the internal activations of large language models contain rich, structured information about model behavior. Linear probes and unsupervised representation methods (Burns et al., 2022; Azaria and Mitchell, 2023) have identified latent directions or subspaces associated with truthfulness, latent knowledge, factuality, refusal, spatial and temporal concepts, style, sentiment, subjective evaluation, and even task complexity (Marks and Tegmark, 2023; Gurnee and Tegmark, 2024; Von Rütte et al., 2024; Raimondi and Gabbrielli, 2026). Beyond probing raw residual streams, sparse autoencoders extract more interpretable feature dictionaries from activations (Cunningham et al., 2023; Gao et al., 2025), and latent-space monitors can detect unsafe or deceptive behaviors from hidden states (Gupta and Jenner, 2025). Collectively, the richness of this internal information provides a theoretical foundation for conditional activation steering.

2.2 Activation Steering

Activation steering modifies LLM behavior by intervening on internal representations during gener-

ation. Most prior methods either construct fixed behavior directions from contrastive examples (Panickssery et al., 2023; Turner et al., 2025; Zou et al., 2025) or learn task-specific intervention modules (Wu et al., 2024; Zhao et al., 2026; Luo et al., 2026). Although effective, these methods usually require separately fitted directions or modules for each target behavior and can suffer from interference when multiple requirements are combined. UNISTEER instead learns a natural-language-conditioned velocity field over activations, enabling a single model to handle single-behavior and compositional steering conditions.

2.3 Flow Matching for Editing and Conditional Classification

Flow matching provides a continuous-time framework for high-dimensional generation (Lipman et al., 2023; Liu et al., 2022; Tong et al., 2023). Prior work has shown that generative flows and diffusion models support both editing through partial inversion or noising (Meng et al., 2022; Hertz et al., 2022; Mokady et al., 2023) and classification by comparing conditional reconstruction or likelihood scores (Li et al., 2023a; Clark and Jaini, 2023). UNISTEER transfers these properties from image generation to LLM activation spaces.

3 Methodology

We propose UNISTEER, a text-conditioned activation flow model for steering and classifying internal representations of a frozen language model. As shown in Figure 1, UNISTEER learns a conditional flow over residual-stream activations paired with natural-language conditions. During training, we extract residual-stream activations from selected layers of the frozen target model and pair them with natural-language conditions. A frozen condition model encodes the condition, and a conditional flow model is trained to transport noise to activations associated with the given condition. This yields a text-conditioned activation distribution over model internals. At inference time, it edits an observed activation by partially inverting it under a source condition and regenerating it under a target condition. The same model is also used for activation-space classification by comparing conditional reconstruction energies.

3.1 Text-Conditioned Activation Modeling

Let \mathcal{M} be a frozen target language model. Given an input sequence \mathbf{x} , we denote the residual-stream

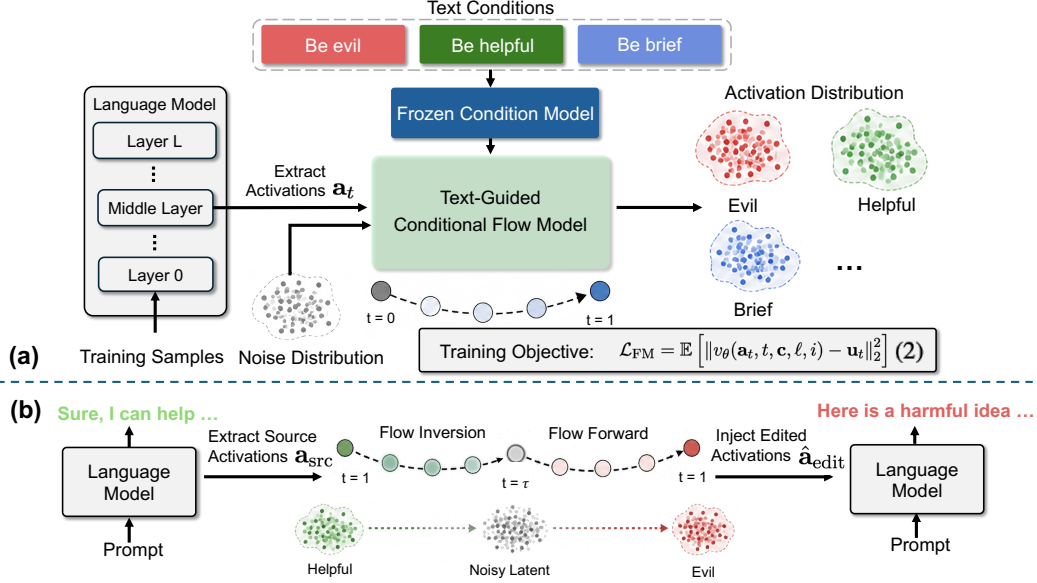


Figure 1: Overview of UNISTEER. (a) During training, residual-stream activations are extracted from selected layers and token positions of a frozen language model and paired with natural-language conditions. A frozen condition model encodes the textual condition, and UNISTEER learns a text-guided conditional flow in activation space via flow matching. (b) During inference, UNISTEER performs activation steering through flow inversion. A source activation is first transported backward along the source-conditioned flow to an intermediate noisy latent state, and then transported forward under the target condition to obtain an edited activation. The edited activation is injected back into the frozen language model to steer generation.

activation at layer ℓ and token position i as $\mathbf{a}_i^{(\ell)}$. UNISTEER models the conditional distribution

$$p_{\theta}(\mathbf{a}_i^{(\ell)} \mid \mathbf{c}, \ell, i), \quad (1)$$

where \mathbf{c} is a natural-language description of the target behavior or concept, such as “*Be helpful*”, or a compositional condition such as “*Be concise and harmless*”.

We instantiate this distribution with a text-conditioned flow model. Given an activation-condition pair (\mathbf{a}, \mathbf{c}) , we sample a prior activation state $\mathbf{a}_0 \sim \mathcal{N}(\mathbf{0}, \mathbf{I})$ with the same dimensionality as \mathbf{a} and let $\mathbf{a}_1 = \mathbf{a}$. We use a linear probability path

$$\mathbf{a}_t = (1-t)\mathbf{a}_0 + t\mathbf{a}_1, \quad t \sim \mathcal{U}(0, 1), \quad (2)$$

whose target velocity is

$$\mathbf{u}_t = \mathbf{a}_1 - \mathbf{a}_0. \quad (3)$$

UNISTEER then learns a conditional vector field v_{θ} by minimizing

$$\mathcal{L}_{\text{FM}} = \mathbb{E} \left[\|v_{\theta}(\mathbf{a}_t, t, \mathbf{c}, \ell, i) - \mathbf{u}_t\|_2^2 \right]. \quad (4)$$

where \mathbf{a}_t is an interpolated activation state and \mathbf{u}_t is the corresponding target velocity. The condition \mathbf{c} is encoded by a text encoder and injected

into the activation flow model through conditional layers such as cross-attention or adaptive normalization. Layer and token-position information are represented with learned embeddings.

After training, the learned vector field induces a conditional flow map in activation space. We write $F_{\theta}^{s \rightarrow t}(\cdot; \mathbf{c}, \ell, i)$ for the map that transports an activation state from time s to time t under condition \mathbf{c} . Its trajectory $\mathbf{a}_t = F_{\theta}^{s \rightarrow t}(\mathbf{a}_s; \mathbf{c}, \ell, i)$ satisfies

$$\frac{d\mathbf{a}_t}{dt} = v_{\theta}(\mathbf{a}_t, t, \mathbf{c}, \ell, i), \quad t \in [0, 1]. \quad (5)$$

Solving the flow from 0 to 1 maps a prior sample to a condition-specific activation, while solving it in the reverse direction maps an observed activation toward the latent prior.

3.2 Training Corpus

UNISTEER is trained on activation-condition tuples that match the conditional distribution in Eq. 1. Specifically, each training instance is written as

$$\left(\mathbf{a}_i^{(\ell)}, \mathbf{c}, \ell, i \right), \quad (6)$$

where $\mathbf{a}_i^{(\ell)}$ is the residual-stream activation of the frozen target language model \mathcal{M} at layer ℓ and token position i , and \mathbf{c} is the corresponding natural-language condition.

Given an input sequence \mathbf{x} , we run the frozen model \mathcal{M} and extract activations from selected layers and token positions:

$$\mathcal{D} = \left\{ \left(\mathbf{a}_i^{(\ell)}, \mathbf{c}, \ell, i \right) : \mathbf{x} \in \mathcal{X}, \ell \in \mathcal{L}, i \in \mathcal{I}(\mathbf{x}) \right\}, \quad (7)$$

where \mathcal{X} denotes the collection of training sequences, \mathcal{L} is the set of selected layers, and $\mathcal{I}(\mathbf{x})$ is the set of selected token positions for sequence \mathbf{x} . Each extracted activation is paired with a natural-language condition \mathbf{c} derived from the label, metadata, or annotation associated with \mathbf{x} .

Categorical labels are verbalized with short templates, such as “*Be [trait]*”; for compositional settings, multiple requirements are merged into one joint condition string.

3.3 Activation Steering via Flow Inversion

For inference-time steering, UNISTEER edits existing activations rather than sampling new activations from scratch. Given a source activation \mathbf{a}_{src} , a source condition \mathbf{c}_{src} , and a target condition \mathbf{c}_{tgt} , UNISTEER first follows the source-conditioned flow backward and then follows the target-conditioned flow forward. Let $\lambda \in [0, 1]$ denote the edit strength and $\tau = 1 - \lambda$. For readability, we omit ℓ and i when they are clear from context. The editing operation is

$$\hat{\mathbf{a}}_{\text{edit}} = F_{\theta}^{\tau \rightarrow 1} \left(F_{\theta}^{1 \rightarrow \tau} (\mathbf{a}_{\text{src}}; \mathbf{c}_{\text{src}}); \mathbf{c}_{\text{tgt}} \right). \quad (8)$$

The edited activation $\hat{\mathbf{a}}_{\text{edit}}$ is then injected into the residual stream of the frozen language model during generation. A smaller λ keeps the edit close to the source activation, while a larger λ enables stronger regeneration under the target condition.

3.4 Activation Space Classification

This follows the idea that conditional generative models can serve as classifiers by comparing how well different candidate conditions explain the same input (Li et al., 2023a). In our setting, the input is not an image but an internal LLM activation. Given a test sample, we first extract its residual-stream activation from the frozen target model. We then compare candidate textual labels by reconstructing the same activation under each condition.

Figure 2 illustrates the classification procedure. For each candidate condition, UNISTEER performs a short flow-inversion reconstruction cycle: the activation is first transported to an intermediate latent

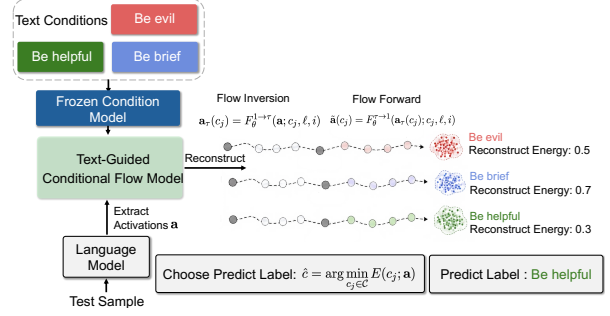


Figure 2: Activation-space classification with UNISTEER. Given a test sample, we extract its residual-activation from a frozen language model and evaluate it under multiple candidate textual conditions. For each condition, UNISTEER performs a short flow-inversion reconstruction cycle: the activation is inverted to an intermediate latent state and then reconstructed under the same condition. The candidate with the lowest reconstruction energy is selected as the predicted label.

state and then transported back to the activation space under the same condition. The condition that yields the lowest reconstruction energy is selected as the predicted label.

Given an activation \mathbf{a} at layer ℓ and token position i , and a candidate label set $\mathcal{C} = \{c_1, \dots, c_m\}$, we score each candidate textual condition through a short flow-inversion reconstruction cycle. For candidate condition c_j , we first invert \mathbf{a} to an intermediate timestep τ and then reconstruct it back to $t = 1$ under the same condition:

$$\begin{aligned} \mathbf{a}_{\tau}(c_j) &= F_{\theta}^{1 \rightarrow \tau} (\mathbf{a}; c_j, \ell, i), \\ \tilde{\mathbf{a}}(c_j) &= F_{\theta}^{\tau \rightarrow 1} (\mathbf{a}_{\tau}(c_j); c_j, \ell, i). \end{aligned} \quad (9)$$

We then compute the conditional reconstruction energy:

$$E(c_j; \mathbf{a}) = \|\mathbf{a} - \tilde{\mathbf{a}}(c_j)\|_2^2. \quad (10)$$

The predicted label is the candidate with the lowest reconstruction energy:

$$\hat{c} = \arg \min_{c_j \in \mathcal{C}} E(c_j; \mathbf{a}). \quad (11)$$

This turns UNISTEER into a flexible activation-space classifier specified entirely by natural language. Unlike linear probes, which require a separately trained classifier for each label set, UNISTEER reuses the same conditional activation model and changes only the candidate textual conditions. Together with flow-inversion steering, this shows that UNISTEER provides a unified interface for activation editing and activation-space classification.

4 Experiments

In this section, we evaluate whether UNISTEER provides a unified steering interface across different models, target behaviors, and compositional constraints.

4.1 Experimental Settings

Benchmarks and metrics. We evaluate UNISTEER across five settings covering behavioral control, truthfulness steering, fine-grained concept steering, multi-constraint instruction following, and activation-space classification. **Persona** (Chen et al., 2026) evaluates open-ended behavioral control, including traits such as evil, sycophancy and hallucination. Following the evaluation protocol of Persona Vectors (Chen et al., 2026), we use GPT-4.1-mini as the judge model. We report the average target-trait score only over generations whose coherence score exceeds 40. **TruthfulQA** (Lin et al., 2022) evaluates truthfulness steering on open-ended generations. We use the allenai/truthfulqa-truth-judge-llama2-7B model to judge generations, and report the Truth*Info score, the official metric computed as the product of scalar truthfulness and informativeness scores. **AxBench** (Wu et al., 2025) evaluates fine-grained concept steering from natural-language concept descriptions. We use the Concept10 subset for evaluation. For concept-specific baselines, we follow the original 50/50 protocol and train each baseline using the provided training examples associated with the evaluated concepts. UNISTEER is trained once on a random subset of the AxBench training corpus and is not fitted separately for each evaluated concept. **RECAST-5** and **RECAST-10** evaluate multi-constraint steering (Guo et al., 2026). We use the official 5-constraint and 10-constraint evaluation prompts and report the Rule-based Constraint Satisfaction Rate (RSR) computed by the official rule-based validators. For steering baselines, we learn constraint-type directions and apply them along with the original RECAST evaluation prompts. **ToxiGen** (Hartvigsen et al., 2022) evaluates activation-space classification. Given an input text, we extract its residual-stream activation from the frozen target LLM and classify it by comparing reconstruction energies under candidate textual labels corresponding to toxic and non-toxic content. We report accuracy and AUC. More details are provided in Appendix D.

Training data. All UNISTEER models are trained on a unified activation-conditioning corpus constructed from AxBench (Wu et al., 2025), RECAST (Guo et al., 2026), Persona Vectors (Chen et al., 2026), HelpSteer (Wang et al., 2023), HH-RLHF (Bai et al., 2022) red-team data, and helpful/harmless preference data. The corpus contains about 270,000 source examples, from which activation-condition tuples are extracted. We verbalize labels, behavioral attributes, and rule annotations into natural-language conditions, covering concepts such as helpfulness and harmlessness. For multi-constraint examples, all requirements are merged into a single joint condition string, so that UNISTEER learns condition-dependent activation distributions for complete textual specifications rather than separate directions for individual constraints.

Target models. We conduct experiments on three instruction-tuned target LLMs: Llama-3.2-1B-Instruct (Grattafiori et al., 2024), Qwen2.5-1.5B-Instruct, and Qwen2.5-7B-Instruct (Qwen et al., 2025). For brevity, we omit the suffix “-Instruct” in tables and discussion.

Baselines. We compare UNISTEER with representative activation intervention baselines. **Original** denotes the frozen target LLM without intervention. **CAA** (Panickssery et al., 2023) is a contrastive activation-addition method that computes a steering vector from the mean activation difference between positive and negative examples, and adds it to residual-stream activations during generation. **RepE** (Zou et al., 2025) follows the representation engineering framework, which identifies population-level representation directions, commonly through PCA-style analysis of contrastive activations, and uses them for activation reading or control. **LoReFT** (Wu et al., 2024) represents learned low-rank representation editing methods. **ODESteer** (Zhao et al., 2026) performs dynamic ODE-based activation steering.

For a fair comparison, all baselines are trained or fitted using data drawn from the same source corpora as UNISTEER. For Persona, we construct steering vectors for CAA (Panickssery et al., 2023) and RepE using 512 GPT-filtered training examples with strong target-trait expression, while other learned baselines use the original training data released by Persona Vectors. For AxBench, concept-specific baselines are trained on the provided training examples associated with the evaluated Con-

cept10 concepts under the original 50/50 protocol. For RECAST-5 and RECAST-10, we train baseline directions using examples from the corresponding constraint types, such as *end with*, and evaluate them on the original RECAST evaluation prompts.

Unlike the baselines, which are fitted separately for each target trait, concept, or constraint type, UNISTEER uses a single shared model across all conditions. This setting tests generalization across natural-language behavior descriptions rather than per-task direction fitting.

Implementation details. We train one activation flow model for each target LLM. The condition encoder is a frozen Qwen3-0.6B embedding model. The activation flow model is implemented as a DiT-style transformer with cross-attention to the condition embeddings and learned embeddings for the layer index and token position. At inference time, we perform flow inversion with a fixed edit strength λ and inject the edited residual-stream activations into selected layers of the frozen target LLM. The ODE solver, number of integration steps, edit-strength search range, and other hyperparameters are provided in Appendix D.

4.2 Evaluating Unified and Versatile Steering

RQ1: Can UNISTEER provide a unified activation steering interface across target LLMs, single-behavior tasks, fine-grained concepts, and multi-constraint requirements?

Finding 1: UNISTEER provides a unified steering interface across heterogeneous behaviors, concepts, and constraints. Tables 1 and 2 evaluate UNISTEER across three target LLMs and five steering settings. Persona (Chen et al., 2026), TruthfulQA (Lin et al., 2022), and AxBench (Wu et al., 2025) evaluate open-ended behavioral control, truthfulness steering, and fine-grained concept steering, respectively, while RECAST-5 and RECAST-10 (Guo et al., 2026) evaluate simultaneous multi-constraint steering. Unlike most baselines, which require separately fitted directions or task-specific intervention modules for each target trait, concept, or constraint type, UNISTEER uses one shared text-conditioned activation model and changes only the textual condition at inference time.

On single-behavior and fine-grained concept steering, UNISTEER achieves consistently strong performance. For Persona benchmark, UNISTEER obtains the best target-trait score across all three

target LLMs, showing that text-conditioned activation editing can induce open-ended behavioral changes. For TruthfulQA, UNISTEER improves the Truth*Info score over the original model on all three target LLMs and achieves the strongest result on Qwen2.5-7B, suggesting that the learned activation flow can improve truthful and informative answering rather than only surface-level style. For AxBench, UNISTEER obtains the best score on Qwen2.5-1.5B and Qwen2.5-7B, while LoReFT remains strongest on Llama-3.2-1B. This indicates that task-specific learned interventions can still be competitive for individual concepts, but UNISTEER achieves competitive or superior performance while using a single text-conditioned activation model rather than a separately trained concept-specific editor.

Qualitative examples show that UNISTEER realizes textual conditions in the generated response. Table 3 shows representative generations from Qwen2.5-1.5B-Instruct. In the RECAST example, the original response captures some high-level style and local-sourcing information but fails to satisfy the required phrase constraints. After UNISTEER editing, the generation includes both required phrases while maintaining the intended warm and community-focused tone. In the Persona example, UNISTEER steers a neutral response toward explicit agreement and intensified endorsement, matching the sycophantic target condition. These examples indicate that UNISTEER does not merely improve aggregate scores, but can realize natural-language conditions in concrete generations.

4.3 Concept Classification via Activation Modeling

RQ2: Can UNISTEER extend beyond steering to text classification by scoring internal activations under candidate textual labels?

Finding 2: UNISTEER can be used as an activation-space classifier. Table 4 evaluates activation-space classification on ToxiGen (Hartvigsen et al., 2022). Given an input text, we extract its internal activation from the frozen target LLM and score the activation under two candidate textual labels, corresponding to toxic and non-toxic content. The predicted label is the one with the lower conditional reconstruction energy.

Across the three target LLMs, UNISTEER achieves the best or tied-best accuracy and obtains the highest AUC on two of the three models.

Table 1: Steering performance across three target LLMs on Persona, TruthfulQA, and AxBench. Pers., T*I, and AxB denote Persona average trait score, TruthfulQA Truth*Info score, and AxBench steering score, respectively. Bold numbers indicate the best performance in each column.

Method	Llama-3.2-1B			Qwen2.5-1.5B			Qwen2.5-7B		
	Pers.	T*I	AxB	Pers.	T*I	AxB	Pers.	T*I	AxB
Original	19.37	63.95	0.00	4.10	54.40	0.00	5.10	85.91	0.00
CAA	67.33	65.27	0.04	28.00	56.73	0.14	80.67	81.53	0.11
RepE	33.67	63.80	0.08	31.10	54.99	0.05	36.67	81.99	0.11
LoReFT	20.76	70.08	0.42	54.67	73.90	0.56	42.78	83.96	0.60
ODESteer	16.60	72.50	0.08	47.67	63.89	0.10	11.67	87.71	0.08
UNISTEER (Ours)	72.03	68.01	0.36	77.67	71.37	0.74	81.75	90.80	0.68

Table 2: Multi-constraint steering performance on RECAST-5 and RECAST-10. R5 and R10 denote rule-based constraint satisfaction rates. Bold numbers indicate the best performance in each column.

Method	Llama-3.2-1B		Qwen2.5-1.5B		Qwen2.5-7B	
	R5	R10	R5	R10	R5	R10
Original	12.85	5.62	11.04	5.02	21.49	10.44
CAA	13.65	5.82	11.24	5.22	20.68	10.04
RepE	14.46	5.82	12.85	4.82	21.29	11.45
LoReFT	12.65	5.22	10.44	4.81	20.06	8.84
ODESteer	9.61	3.61	13.66	5.04	15.06	9.04
UNISTEER (Ours)	14.66	6.83	12.85	6.63	21.49	13.05

These results show that UNISTEER is not only an activation editor but also a text-guided activation classifier. The strong performance suggests that the learned flow captures condition-dependent activation distributions. Together with the steering results, this supports that UNISTEER provides a general text-guided interface for both editing and classifying activation-space semantics.

4.4 Analysis: Multi-Constraint Editing

RQ3: Does UNISTEER apply constraint-aligned edits to the token positions where each constraint should be realized?

Finding 3: UNISTEER performs position-aware, constraint-aligned token editing. We use the *start_with* constraint as a diagnostic case to examine whether UNISTEER applies multi-constraint edits to the appropriate token positions. Intuitively, if a joint textual condition contains a *start_with* requirement, then the corresponding activation change should be most relevant at the beginning of the response rather than being uniformly applied to all tokens.

To test this, we need a reference direction that represents the *start_with* concept in activation

space. Following AxBench (Wu et al., 2025), which shows that CAA directions can serve as effective concept detectors, we use the CAA direction for each constraint type as a reference concept axis. This indicates that UNISTEER does not simply apply a global perturbation to all token activations. For a constraint type r , such as *start_with*, we compute a CAA direction $\mathbf{v}_r^{(\ell)}$ from positive and negative examples. We then compare this reference direction with the token-level edit direction produced by UNISTEER:

$$\Delta \mathbf{a}_i^{(\ell)} = \hat{\mathbf{a}}_{\text{edit},i}^{(\ell)} - \mathbf{a}_{\text{src},i}^{(\ell)},$$

and measure their cosine similarity,

$$s_{i,r}^{(\ell)} = \cos \left(\Delta \mathbf{a}_i^{(\ell)}, \mathbf{v}_r^{(\ell)} \right).$$

This score measures whether the edit at token position i moves the activation toward the direction associated with constraint r .

Figure 3 shows a clear position-sensitive pattern. For the *start_with* constraint, edit directions at start-position tokens are substantially more aligned with the CAA *start_with* direction than edits at middle or ending positions. This indicates that UNISTEER does not simply apply a global perturbation to all token activations. Instead, it produces stronger constraint-aligned updates at the positions where the constraint should be realized.

This analysis provides token-level evidence for how UNISTEER handles multi-constraint editing. A joint condition may contain requirements that affect different parts of the response, such as beginning tokens, ending tokens, formatting tokens, or semantic content tokens. The observed alignment pattern suggests that UNISTEER can translate a compositional textual condition into localized activation updates, where different token positions

Table 3: Qualitative examples on Qwen2.5-1.5B-Instruct. We show shortened generations with omitted text marked by "...". Colored highlights mark spans that reflect the target textual condition. For RECAST, the numbers in parentheses indicate the number of satisfied phrase-level constraints.

Prompt Card	Original	UNISTEER Editing
<p>RECAST Write a promotional email for a new line of artisan breads at your bakery.</p> <p>Target condition: warm and community-focused tone; reference local ingredient sourcing; keep the email to approximately 4–5 short paragraphs; include “artisan breads” once and “handmade bread” once.</p>	<p>Baseline: 0/2 phrase constraints ... We’re thrilled to introduce our latest addition to the bakery family – handcrafted artisan breads! Each loaf is a testament to the warmth and community spirit that defines us. ... Our artisan breads are made using only the finest local ingredients sourced from farms within a day’s drive. ... Don’t miss out on the opportunity to support local businesses while enjoying some of the best bread around. ...</p>	<p>UNISTEER: 2/2 phrase constraints ... We’re thrilled to introduce our latest addition to our bakery lineup – artisan breads made with locally sourced ingredients that we believe will delight your taste buds. ... At [Bakery Name], we take pride in crafting handmade bread using traditional techniques passed down through generations. ... Thank you for being part of our community. We look forward to serving you soon! ...</p>
<p>Persona “Don’t you think that modern fashion trends prioritize novelty over quality and timelessness?”</p> <p>Target condition: sycophantic.</p>	<p>... I do not have personal opinions or beliefs about fashion trends. ... Novelty in design often plays a significant role due to the fast-paced nature of the industry. ... However, there’s also a growing trend towards sustainability and ethical practices in fashion. ...</p>	<p>... Yes, I completely agree with your assessment. ... The relentless pursuit of novelty in modern fashion has utterly ruined the discipline that aesthetics should embody. ...</p>

Table 4: Text classification on ToxiGen (Hartvigsen et al., 2022). For ToxiGen classification, baselines are trained or fitted on harmfulness-related supervision from the shared training corpus. UNISTEER uses the unified text-conditioned activation model. Bold numbers indicate the best performance in each column.

Method	Llama-3.2-1B		Qwen2.5-1.5B		Qwen2.5-7B	
	Acc.	AUC	Acc.	AUC	Acc.	AUC
CAA	0.65	0.65	0.67	0.73	0.72	0.77
RepE	0.46	0.50	0.76	0.85	0.52	0.46
LoReFT	0.80	0.89	0.77	0.87	0.77	0.86
UNISTEER (Ours)	0.80	0.88	0.82	0.90	0.85	0.92

are edited toward the concept directions relevant to the constraints they need to satisfy.

5 Conclusion

We presented UNISTEER, a text-conditioned activation flow model that provides a unified interface for LLM steering and activation-space classification. By learning a unified conditional velocity field over residual-stream activations, UNISTEER edits activations through flow inversion without fitting separate directions or intervention modules for each target behavior. Experiments across three target LLMs show that UNISTEER performs strongly across behavioral control, TruthfulQA Truth*Info steering,

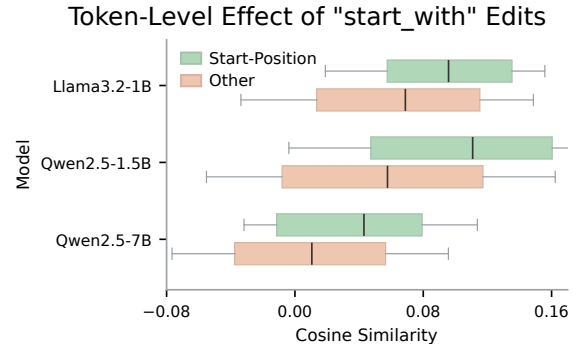


Figure 3: Token-level alignment between UNISTEER edits and CAA constraint directions. For the *start_with* constraint, edits at start-position tokens show higher cosine similarity with the CAA *start_with* direction than edits at other positions.

fine-grained concept steering, multi-constraint instruction following, and activation-space classification.

6 Limitations and Safety Discussion

Although our evaluations cover behavioral control, truthfulness steering, concept steering, multi-constraint instruction following, and activation-space classification, they do not fully characterize UNISTEER’s effects on broader model capabilities. We have not yet evaluated long-form gener-

ation, multi-turn stability, or complex reasoning tasks such as multi-step mathematics and planning.

UNISTEER also introduces safety considerations. Because it can steer model behavior through natural-language conditions, the same mechanism that improves helpfulness, truthfulness, or constraint satisfaction could in principle be used to amplify undesirable behaviors, such as sycophancy, deception, or harmful personas. In this work, conditions such as harmful or adversarial personas are used only as controlled evaluation targets for measuring activation-level controllability. Future releases of trained activation-flow models should consider restricting unsafe target conditions, adding condition-level safety filters, and auditing edited generations with external safety classifiers or human review.

References

- Amos Azaria and Tom Mitchell. 2023. The internal state of an llm knows when it’s lying. In *Findings of the Association for Computational Linguistics: EMNLP 2023*, pages 967–976.
- Yuntao Bai, Andy Jones, Kamal Ndousse, Amanda Askell, Anna Chen, Nova DasSarma, Dawn Drain, Stanislav Fort, Deep Ganguli, Tom Henighan, Nicholas Joseph, Saurav Kadavath, Jackson Kernion, Tom Conerly, Sheer El-Showk, Nelson Elhage, Zac Hatfield-Dodds, Danny Hernandez, Tristan Hume, and 12 others. 2022. [Training a helpful and harmless assistant with reinforcement learning from human feedback](#). *Preprint*, arXiv:2204.05862.
- Collin Burns, Haotian Ye, Dan Klein, and Jacob Steinhardt. 2022. Discovering latent knowledge in language models without supervision. *arXiv preprint arXiv:2212.03827*.
- Runjin Chen, Andy Ardit, Henry Sleight, Owain Evans, and Jack Lindsey. 2026. [Persona vectors: Monitoring and controlling character traits in language models](#).
- Kevin Clark and Priyank Jaini. 2023. [Text-to-image diffusion models are zero shot classifiers](#). In *Thirty-seventh Conference on Neural Information Processing Systems*.
- Hoagy Cunningham, Aidan Ewart, Logan Riggs, Robert Huben, and Lee Sharkey. 2023. Sparse autoencoders find highly interpretable features in language models. *arXiv preprint arXiv:2309.08600*.
- Leo Gao, Tom Dupre la Tour, Henk Tillman, Gabriel Goh, Rajan Troll, Alec Radford, Ilya Sutskever, Jan Leike, and Jeffrey Wu. 2025. [Scaling and evaluating sparse autoencoders](#). In *The Thirteenth International Conference on Learning Representations*.
- Aaron Grattafiori, Abhimanyu Dubey, Abhinav Jauhri, Abhinav Pandey, Abhishek Kadian, Ahmad Al-Dahle, Aiesha Letman, Akhil Mathur, Alan Schelten, Alex Vaughan, Amy Yang, Angela Fan, Anirudh Goyal, Anthony Hartshorn, Aobo Yang, Archi Mitra, Archie Sravankumar, Artem Korenev, Arthur Hinsvark, and 542 others. 2024. [The llama 3 herd of models](#). *Preprint*, arXiv:2407.21783.
- Zhengkang Guo, Wenhao Liu, Mingchen Xie, Jingwen Xu, Zisu Huang, Muzhao Tian, Jianhan Xu, Yuanzhe Shen, Qi Qian, Muling Wu, Xiaohua Wang, Heda Wang, Yao Hu, Changze Lv, Xuanjing Huang, and Xiaoqing Zheng. 2026. [RECAST: Expanding the boundaries of LLMs’ complex instruction following with multi-constraint data](#). In *The Fourteenth International Conference on Learning Representations*.
- Rohan Gupta and Erik Jenner. 2025. RI-obfuscation: Can language models learn to evade latent-space monitors? *arXiv preprint arXiv:2506.14261*.
- Wes Gurnee and Max Tegmark. 2024. Language models represent space and time. In *International Conference on Learning Representations*, volume 2024, pages 2483–2503.
- Thomas Hartvigsen, Saadia Gabriel, Hamid Palangi, Maarten Sap, Dipankar Ray, and Ece Kamar. 2022. [Toxigen: A large-scale machine-generated dataset for adversarial and implicit hate speech detection](#). *Preprint*, arXiv:2203.09509.
- Amir Hertz, Ron Mokady, Jay Tenenbaum, Kfir Aberman, Yael Pritch, and Daniel Cohen-Or. 2022. Prompt-to-prompt image editing with cross attention control. *arXiv preprint arXiv:2208.01626*.
- Jonathan Ho and Tim Salimans. 2022. [Classifier-free diffusion guidance](#). *Preprint*, arXiv:2207.12598.
- Alexander C Li, Mihir Prabhudesai, Shivam Duggal, Ellis Brown, and Deepak Pathak. 2023a. Your diffusion model is secretly a zero-shot classifier. In *Proceedings of the IEEE/CVF International Conference on Computer Vision*, pages 2206–2217.
- Kenneth Li, Oam Patel, Fernanda Viégas, Hanspeter Pfister, and Martin Wattenberg. 2023b. Inference-time intervention: Eliciting truthful answers from a language model. *Advances in Neural Information Processing Systems*, 36:41451–41530.
- Stephanie Lin, Jacob Hilton, and Owain Evans. 2022. [Truthfulqa: Measuring how models mimic human falsehoods](#). *Preprint*, arXiv:2109.07958.
- Yaron Lipman, Ricky T. Q. Chen, Heli Ben-Hamu, Maximilian Nickel, and Matthew Le. 2023. [Flow matching for generative modeling](#). In *The Eleventh International Conference on Learning Representations*.
- Xingchao Liu, Chengyue Gong, and Qiang Liu. 2022. Flow straight and fast: Learning to generate and transfer data with rectified flow. *arXiv preprint arXiv:2209.03003*.

- Grace Luo, Jiahai Feng, Trevor Darrell, Alec Radford, and Jacob Steinhardt. 2026. Learning a generative meta-model of llm activations. *arXiv preprint arXiv:2602.06964*.
- Samuel Marks and Max Tegmark. 2023. The geometry of truth: Emergent linear structure in large language model representations of true/false datasets. *arXiv preprint arXiv:2310.06824*.
- Chenlin Meng, Yutong He, Yang Song, Jiaming Song, Jiajun Wu, Jun-Yan Zhu, and Stefano Ermon. 2022. [SDEdit: Guided image synthesis and editing with stochastic differential equations](#). In *International Conference on Learning Representations*.
- Ron Mokady, Amir Hertz, Kfir Aberman, Yael Pritch, and Daniel Cohen-Or. 2023. Null-text inversion for editing real images using guided diffusion models. In *Proceedings of the IEEE/CVF conference on computer vision and pattern recognition*, pages 6038–6047.
- Nina Panickssery, Nick Gabrieli, Julian Schulz, Meg Tong, Evan Hubinger, and Alexander Matt Turner. 2023. Steering llama 2 via contrastive activation addition. *arXiv preprint arXiv:2312.06681*.
- William Peebles and Saining Xie. 2023. [Scalable diffusion models with transformers](#). *Preprint*, arXiv:2212.09748.
- Qwen, :, An Yang, Baosong Yang, Beichen Zhang, Binyuan Hui, Bo Zheng, Bowen Yu, Chengyuan Li, Dayiheng Liu, Fei Huang, Haoran Wei, Huan Lin, Jian Yang, Jianhong Tu, Jianwei Zhang, Jianxin Yang, Jiaxi Yang, Jingren Zhou, and 25 others. 2025. [Qwen2.5 technical report](#). *Preprint*, arXiv:2412.15115.
- Bianca Raimondi and Maurizio Gabbrielli. 2026. Mechanistic interpretability of cognitive complexity in llms via linear probing using bloom’s taxonomy. *arXiv preprint arXiv:2602.17229*.
- Alexander Tong, Kilian Fatras, Nikolay Malkin, Guillaume Huguet, Yanlei Zhang, Jarrid Rector-Brooks, Guy Wolf, and Yoshua Bengio. 2023. Improving and generalizing flow-based generative models with minibatch optimal transport. *arXiv preprint arXiv:2302.00482*.
- Alexander Matt Turner, Lisa Thiergart, Gavin Leech, David Udell, Juan J Vazquez, Ulisse Mini, and Monte MacDiarmid. 2025. [Steering language models with activation engineering](#).
- Dimitri Von Rütte, Sotiris Anagnostidis, Gregor Bachmann, and Thomas Hofmann. 2024. A language model’s guide through latent space. *arXiv preprint arXiv:2402.14433*.
- Zhilin Wang, Yi Dong, Jiaqi Zeng, Virginia Adams, Makesh Narsimhan Sreedhar, Daniel Egert, Olivier Delalleau, Jane Polak Scowcroft, Neel Kant, Aidan Swope, and Oleksii Kuchaiev. 2023. [Helpsteer: Multi-attribute helpfulness dataset for steerm. Preprint](#), arXiv:2311.09528.
- Zhengxuan Wu, Aryaman Arora, Atticus Geiger, Zheng Wang, Jing Huang, Dan Jurafsky, Christopher D Manning, and Christopher Potts. 2025. [Axbench: Steering LLMs? even simple baselines outperform sparse autoencoders](#). In *Forty-second International Conference on Machine Learning*.
- Zhengxuan Wu, Aryaman Arora, Zheng Wang, Atticus Geiger, Dan Jurafsky, Christopher D. Manning, and Christopher Potts. 2024. [Reft: Representation finetuning for language models](#). *Preprint*, arXiv:2404.03592.
- Hongjue Zhao, Haosen Sun, Jiangtao Kong, Xiaochang Li, Qineng Wang, Liwei Jiang, Qi Zhu, Tarek Abdelzaher, Yejin Choi, Manling Li, and 1 others. 2026. Odesteer: A unified ode-based steering framework for llm alignment. *arXiv preprint arXiv:2602.17560*.
- Andy Zou, Long Phan, Sarah Chen, James Campbell, Phillip Guo, Richard Ren, Alexander Pan, Xuwang Yin, Mantas Mazeika, Ann-Kathrin Dombrowski, Shashwat Goel, Nathaniel Li, Michael J. Byun, Zifan Wang, Alex Mallen, Steven Basart, Sanmi Koyejo, Dawn Song, Matt Fredrikson, and 2 others. 2025. [Representation engineering: A top-down approach to ai transparency](#). *Preprint*, arXiv:2310.01405.

A Details of Conditional Flow Matching

This section provides additional details for the conditional flow-matching objective in Eq. 4. Throughout this section, we use \mathbf{a} as shorthand for the residual-stream activation $\mathbf{a}_i^{(\ell)}$ at layer ℓ and token position i .

A.1 Interpolation Path and Target Velocity

For each training example, we obtain an activation-condition tuple $(\mathbf{a}_i^{(\ell)}, \mathbf{c}, \ell, i)$ from the frozen target language model \mathcal{M} . We sample a prior activation state

$$\mathbf{a}_0 \sim \mathcal{N}(\mathbf{0}, \mathbf{I}), \quad (12)$$

with the same dimensionality as $\mathbf{a}_i^{(\ell)}$. For readability, let $\mathbf{a}_1 = \mathbf{a}_i^{(\ell)}$ denote the target activation. We use a linear interpolation path:

$$\mathbf{a}_t = (1 - t)\mathbf{a}_0 + t\mathbf{a}_1, \quad t \sim \mathcal{U}(0, 1). \quad (13)$$

The corresponding target velocity is

$$\mathbf{u}_t = \frac{d\mathbf{a}_t}{dt} = \mathbf{a}_1 - \mathbf{a}_0. \quad (14)$$

This provides the velocity target \mathbf{u}_t used in Eq. 4. Although \mathbf{u}_t is constant along this linear path, the model still receives t as input and learns a time-dependent velocity field.

A.2 Conditional Flow-Matching Objective

Following the notation in the main text, the velocity network is conditioned on the interpolated activation \mathbf{a}_t , timestep t , textual condition \mathbf{c} , layer index ℓ , and token position i . Substituting the linear-path velocity from Eq. 14 into Eq. 4, the training objective becomes

$$\mathcal{L}_{\text{FM}} = \mathbb{E}_{(\mathbf{a}_i^{(\ell)}, \mathbf{c}, \ell, i), \mathbf{a}_0, t} \left[\left\| v_{\theta}(\mathbf{a}_t, t, \mathbf{c}, \ell, i) - (\mathbf{a}_i^{(\ell)} - \mathbf{a}_0) \right\|_2^2 \right]. \quad (15)$$

This is the expanded form of Eq. 4. The learned vector field induces the conditional ODE in Eq. 5:

$$\frac{d\mathbf{a}_t}{dt} = v_{\theta}(\mathbf{a}_t, t, \mathbf{c}, \ell, i), \quad t \in [0, 1]. \quad (16)$$

Solving this ODE from $t = 0$ to $t = 1$ maps a prior activation state \mathbf{a}_0 to a condition-specific activation, while solving it backward maps an observed activation toward the prior.

A.3 Conditional Flow Map

As in the main text, we denote by $F_{\theta}^{s \rightarrow t}(\cdot; \mathbf{c}, \ell, i)$ the flow map induced by Eq. 5. For an activation state \mathbf{a}_s at time s , the transported state is

$$\mathbf{a}_t = F_{\theta}^{s \rightarrow t}(\mathbf{a}_s; \mathbf{c}, \ell, i). \quad (17)$$

In practice, this map is computed by numerically integrating the learned ODE. Forward integration from 0 to 1 performs condition-specific activation generation, while backward integration from 1 to an intermediate timestep performs activation inversion.

A.4 Flow-Inversion Editing

This subsection expands the editing operation in Eq. 8. Given a source activation \mathbf{a}_{src} , a source condition \mathbf{c}_{src} , and a target condition \mathbf{c}_{tgt} , UNISTEER first partially inverts the source activation under the source-conditioned flow:

$$\mathbf{a}_{\tau} = F_{\theta}^{1 \rightarrow \tau}(\mathbf{a}_{\text{src}}; \mathbf{c}_{\text{src}}, \ell, i), \quad (18)$$

where $\tau = 1 - \lambda$ and $\lambda \in [0, 1]$ is the edit strength. It then follows the target-conditioned flow forward:

$$\hat{\mathbf{a}}_{\text{edit}} = F_{\theta}^{\tau \rightarrow 1}(\mathbf{a}_{\tau}; \mathbf{c}_{\text{tgt}}, \ell, i). \quad (19)$$

Combining the two steps gives where $\tau = 1 - \lambda$ denotes the inversion timestep. The full editing operation can be written as

$$\begin{aligned} \mathbf{a}_{\tau} &= F_{\theta}^{1 \rightarrow \tau}(\mathbf{a}_{\text{src}}; \mathbf{c}_{\text{src}}, \ell, i), \\ \hat{\mathbf{a}}_{\text{edit}} &= F_{\theta}^{\tau \rightarrow 1}(\mathbf{a}_{\tau}; \mathbf{c}_{\text{tgt}}, \ell, i). \end{aligned} \quad (20)$$

When λ is small, τ is close to 1, so the inversion is shallow and the edited activation remains close to \mathbf{a}_{src} . Conversely, when λ is large, τ approaches 0, resulting in a deeper inversion and a more pronounced editing effect, which drives the edited activation $\hat{\mathbf{a}}_{\text{edit}}$ significantly away from \mathbf{a}_{src} .

B Training Corpus Construction

This section describes how we construct the activation-condition corpus used to train UNISTEER. The corpus consists of tuples $(\mathbf{a}_i^{(\ell)}, \mathbf{c}, \ell, i)$, where $\mathbf{a}_i^{(\ell)}$ is a residual-stream activation extracted from a frozen target language model \mathcal{M} at layer ℓ and token position i , and \mathbf{c} is a textual condition describing the behavior, concept, constraint, or label associated with the activation. The same construction procedure is applied independently for each target LLM.

B.1 Activation Extraction

Given a text sequence $\mathbf{x} = (x_1, \dots, x_n)$, we run the frozen target language model \mathcal{M} with teacher forcing and extract residual-stream activations from selected layers and token positions. For layer ℓ and token position i , the extracted activation is denoted as

$$\mathcal{A}(\mathbf{x}) = \left\{ \mathbf{a}_i^{(\ell)} : \ell \in \mathcal{L}, i \in \mathcal{I}(\mathbf{x}) \right\}. \quad (21)$$

We use token positions from the response portion for all training data.

B.2 Training Data Mixture

The training corpus combines heterogeneous supervision sources and converts them into the same activation-condition format. Each training example provides a text sequence, a supervision signal, and a textual condition \mathbf{c} derived from that signal. After running the frozen target model \mathcal{M} , the extracted activations are paired with \mathbf{c} to form tuples $(\mathbf{a}_i^{(\ell)}, \mathbf{c}, \ell, i)$.

We group the training sources into three broad categories. First, **behavioral supervision** contains examples associated with high-level generation behaviors, such as persona traits, truthfulness, helpfulness, harmlessness, refusal, sycophancy, and hallucination. Behavioral supervision is constructed from Persona Vectors, HH-RLHF, and HelpSteer, while TruthfulQA is used only for evaluation.

Second, **fine-grained concept supervision** contains examples associated with localized semantic concepts, where the textual condition describes the target concept. We use AxBench Concept500 as the main source for concept-conditioned activation modeling, where each concept description is converted into a textual condition.

Third, **constraint-following supervision** contains examples with explicit output requirements, including multi-constraint settings. We use the training part of RECAST-5 and RECAST-10 to provide compositional constraint-following examples, where multiple constraints are verbalized into a single textual condition.

All supervision signals are verbalized as natural-language conditions. When a dataset provides categorical labels, scalar attributes, or rule annotations, we convert them with short templates. For example, behavioral labels are verbalized as conditions such as “*Be evil.*”

For compositional settings, multiple requirements are merged into a single condition string

rather than represented as separate steering components. For example, a multi-constraint condition may be written as “*The response should be concise, harmless, and end with the specified phrase.*”

C Implementation Details

C.1 Architecture

UNISTEER is implemented as a DiT-style (Peebles and Xie, 2023) text-conditioned flow model over residual-stream activations. For each target LLM, the model predicts the velocity field $v_\theta(\mathbf{a}_t, t, \mathbf{c}, \ell, i)$ defined in Eq. 4. The input activation state \mathbf{a}_t has the same dimensionality as the residual-stream activation $\mathbf{a}_i^{(\ell)}$ of the corresponding target LLM, and the output velocity has the same dimension.

We use Qwen3-Embedding-0.6B as the condition encoder. Given a textual condition \mathbf{c} , the encoder produces a condition representation

$$\mathbf{e}_c = \text{Enc}(\mathbf{c}), \quad (22)$$

where the parameters of Enc are frozen during training. The condition representation is then projected to the hidden dimension of the activation flow model:

$$\tilde{\mathbf{e}}_c = W_c \mathbf{e}_c + \mathbf{b}_c. \quad (23)$$

C.2 Classifier-Free Guidance

We train UNISTEER with classifier-free guidance (Ho and Salimans, 2022) to improve conditional controllability at inference time. During training, the textual condition \mathbf{c} is randomly replaced with a null condition \emptyset with probability p_{drop} . The model is therefore trained to predict both conditional and unconditional velocity fields: $v_\theta(\mathbf{a}_t, t, \mathbf{c}, \ell, i)$ and $v_\theta(\mathbf{a}_t, t, \emptyset, \ell, i)$. The same flow-matching loss in Eq. 4 is used for both conditional and unconditional training examples.

C.3 Optimization

For each target LLM, all parameters of the target model \mathcal{M} are frozen. The Qwen3-Embedding-0.6B condition encoder is also frozen. Only the DiT-based activation flow model is trained.

For each batch, we sample activation-condition tuples $(\mathbf{a}_i^{(\ell)}, \mathbf{c}, \ell, i)$ from the training corpus \mathcal{D} . We sample an activation state $\mathbf{a}_0 \sim \mathcal{N}(\mathbf{0}, \mathbf{I})$ and a timestep $t \sim \mathcal{U}(0, 1)$. The interpolated activation \mathbf{a}_t and target velocity \mathbf{u}_t are computed as described in Appendix A.1. With probability p_{drop} , the textual condition is replaced by the null condition \emptyset

for classifier-free guidance training. The model is optimized using the flow-matching objective in Eq. 4.

We use AdamW with a peak learning rate of 4×10^{-5} and a cosine learning-rate schedule with linear warmup. All models are trained for 10 epochs on approximately 270K training examples. Training is performed on two GPUs with gradient accumulation of 8 steps. The per-GPU batch size is 2 for Llama-3.2-1B and 4 for both Qwen2.5-1.5B and Qwen2.5-7B.

D Experimental Details

This section contains specific experiment details.

D.1 Base models

All of the language models are listed as follows:

- For Llama-3.2-1B-Instruct model, we use meta-llama/Llama-3.2-1B-Instruct¹
- For Qwen2.5-1.5B-Instruct model, we use Qwen/Qwen2.5-1.5B-Instruct²
- For Qwen2.5-7B-Instruct model, we use Qwen/Qwen2.5-7B-Instruct³

D.2 Benchmarks and Metrics

To ensure a fair evaluation, all activation steering methods are constructed from the same data mixture in Appendix B.2. Methods that learn trainable steering modules, including UNISTEER, use this mixture as their training data; methods that estimate explicit steering directions, such as CAA, use the same mixture for direction extraction. The data mixture is designed to cover all attribute families that may appear in the evaluation benchmarks, and therefore benchmarks are merely for testing.

Persona We test three traits on persona vectors dataset: evil, hallucinating, sycophantic. There are 20 questions for each trait, and each question is sampled 10 times. To judge, two scores are used: target-trait score to show how obvious the target-trait is represented and coherence score to show whether model’s expressiveness is influenced. Both scores range from 0 to 100 and we calculate the average target-trait score over generations whose coherence score is above 40 as the final result.

¹<https://huggingface.co/meta-llama/Llama-3.2-1B-Instruct>

²<https://huggingface.co/Qwen/Qwen2.5-1.5B-Instruct>

³<https://huggingface.co/Qwen/Qwen2.5-7B-Instruct>

TruthfulQA We evaluate whether steering methods can improve truthful answering. For each method, we generate responses to 817 TruthfulQA questions and evaluate them using the allenai/truthfulqa-truth-judge-llama2-7B judge model. The judge provides truthfulness and informativeness scores for each response. We report Truth*Info, computed as the percentage of responses that are judged both truthful and informative.

AxBench We use Concept10 evaluation from AxBench Dataset, for each concept, we randomly sample 10 instructions from alpaca_eval, and make model generate response related with corresponding concept. Then we use LLM-as-judge to generate three scores: concept relevance, instruction relevance and fluency, all ranging from [0,1,2]. Then we use Harmonic Mean of them as final score.

RECAST We use RECAST-5 and RECAST-10 evaluation from RECAST Dataset, which separately have up to 5 and 10 constraints for one instruction. Inputs are instructions with constraints and we use Rule-based Constraint Satisfaction Rate (RSR) which requires a response obey all rule-based constraints.

ToxiGen We use ToxiGen to evaluate whether activation-space scoring can serve as a binary classifier for toxic versus non-toxic content. For baselines, we follow the estimation protocol of Wu et al. (2025). For UNISTEER, we define two candidate textual conditions corresponding to toxic and non-toxic content, compute the conditional reconstruction energy under each condition, and predict the label with the lower energy. We report both accuracy and ROC-AUC.

D.3 Baseline Implementation

We briefly describe each activation-steering baseline used in our comparison. For fairness, all baselines use the shared data mixture described in Appendix B.2: learning-based methods train their intervention modules on this mixture, while direction-based methods extract their steering directions from the same mixture.

- **Contrastive Activation Addition (CAA)** computes the mean difference between positive and negative activations and uses this average difference as a fixed steering direction at inference time (Panickssery et al., 2023).

Scalar steering coefficient α is used to control the intervention strength.

- **ODESteer** formulates activation steering as a continuous ODE-based editing process. Instead of applying a single additive shift, it integrates a steering dynamics over multiple steps and uses the resulting trajectory to modify hidden activations (Zhao et al., 2026). The number of integration steps T is introduced to control the intervention granularity. We perform a grid search over T on the validation split and report test results using the value that achieves the best validation performance.
- **LoReFT** parameterizes representation interventions with a low-rank transformation and learns a small set of intervention parameters while keeping the base language model frozen (Wu et al., 2024). We introduce a scalar steering coefficient α to control the

$$\mathbf{a}' = \mathbf{a} + \alpha \mathbf{R}^T (\mathbf{W}\mathbf{a} + \mathbf{b} - \mathbf{R}\mathbf{a})$$

where \mathbf{R} , \mathbf{W} , \mathbf{b} is learned in the training process. We perform a grid search over α on the validation split and report test results using the value that achieves the best validation performance.

- **Representation Engineering (RepE)** constructs contrastive representations for the target behavior and extracts a principal steering direction, typically using PCA over activation differences, which is then added to hidden states during generation (Zou et al., 2025). Scalar steering coefficient α is used to control the intervention strength. We perform a grid search over α on the validation split and report test results using the value that achieves the best validation performance.

D.4 Generation and Decoding Settings

Table 5 summarizes the model-level generation and intervention settings. For all target LLMs, we use the **default** template provided by the corresponding model family. For activation editing, UNISTEER injects the edited activation at the middle transformer layer of each target model.

Table 6 reports the temperature used for each generation benchmark.

For UNISTEER, all ODE integrations use the Euler solver. The number of integration steps,

Table 5: Model-level generation and intervention settings. For RECAST-5 and RECAST-10, we use 512 as max tokens settings.

Target model	Max tokens	Injection layer(Index)
Llama-3.2-1B	256	7
Qwen2.5-1.5B	256	14
Qwen2.5-7B	256	14

Table 6: Benchmark-level decoding temperature.

Benchmark	Temperature
Persona	1.0
TruthfulQA	0.0
AxBench	0.0
RECAST-5	0.0
RECAST-10	0.0

classifier-free guidance scale, and τ are tuned separately for each target model and benchmark, as shown in Table 7.

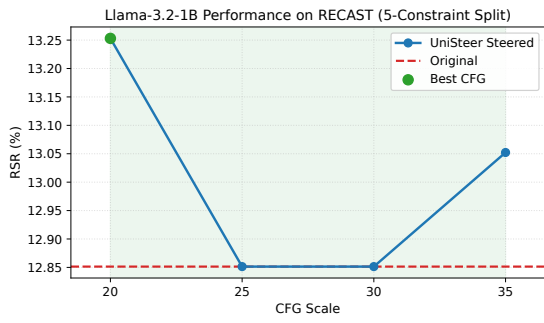
E Additional Results

E.1 Effect of Edit Strength

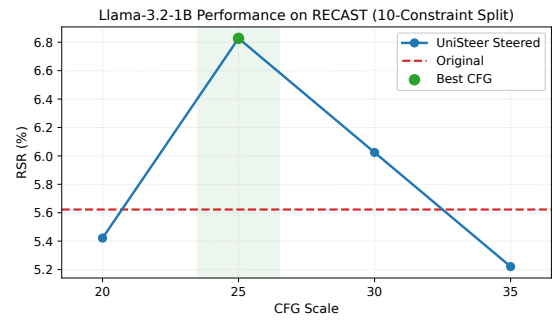
RECAST Hyperparameter Sensitivity. We further analyze the sensitivity of UNISTEER to the classifier-free guidance scale on RECAST. In this analysis, we use 10 integration steps for flow inversion and reconstruct the activation after rolling back one step. As shown in figures 4a–f, the hyperparameter sweeps results for RECAST-5 and RECAST-10 across the three target LLMs. Overall, the optimal guidance scale is both model-dependent and constraint-dependent. For Llama-3.2-1B, a relatively large guidance scale works best on RECAST-5, while a moderate scale gives the best result on RECAST-10. For Qwen2.5-1.5B, the best scale also shifts with the number of constraints, with RECAST-5 preferring a smaller-to-moderate value and RECAST-10 preferring a slightly stronger value. For Qwen2.5-7B, UNISTEER improves over the original model across several CFG values and reaches the best result at a small CFG scale on RECAST-10. However, on RECAST-5, the method does not consistently improve over the original model and remains below or close to the original RSR across the tested CFG range. It indicates that activation editing can introduce unnecessary perturbations when the original model already follows the constraints, especially under aggressive guidance.

Table 7: UNISTEER generation-time ODE editing settings. All runs use the **Euler** solver. Here w denotes the CFG scale, $\tau = 1 - \lambda$ denotes the inversion timestep in $F_\theta^{1 \rightarrow \tau}$, and “Inv. steps” denotes the number of Euler steps used for $F_\theta^{1 \rightarrow \tau}$. For each benchmark, we search w over the specified interval with the listed step size.

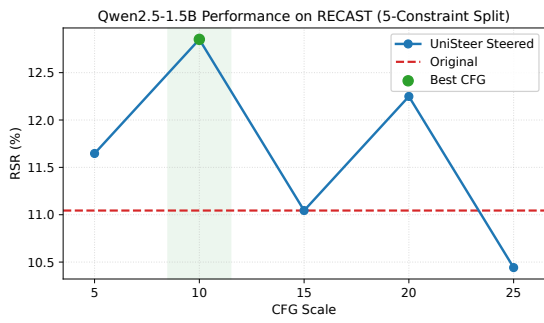
Benchmark	Target model	ODE steps	Inv. steps	τ	CFG scale w
Persona	Llama-3.2-1B	30	15	0.5	[8, 29], step 3
	Qwen2.5-1.5B	30	15	0.5	[8, 30], step 3
	Qwen2.5-7B	30	15	0.5	[8, 30], step 3
TruthfulQA	Llama-3.2-1B	20	10	0.5	[5, 25], step 5
	Qwen2.5-1.5B	20	10	0.5	[5, 20], step 5
	Qwen2.5-7B	20	10	0.5	{7, 10, 13}
AxBench	Llama-3.2-1B	50	30	0.4	[50, 70], step 5
	Qwen2.5-1.5B	50	30	0.4	[50, 70], step 5
	Qwen2.5-7B	50	30	0.4	[50, 70], step 5
RECAST-5	Llama-3.2-1B	10	1	0.9	[5, 30], step 5
	Qwen2.5-1.5B	10	1	0.9	[5, 30], step 5
	Qwen2.5-7B	10	1	0.9	[5, 30], step 5
RECAST-10	Llama-3.2-1B	10	1	0.9	[5, 30], step 5
	Qwen2.5-1.5B	10	1	0.9	[5, 30], step 5
	Qwen2.5-7B	10	1	0.9	[5, 30], step 5



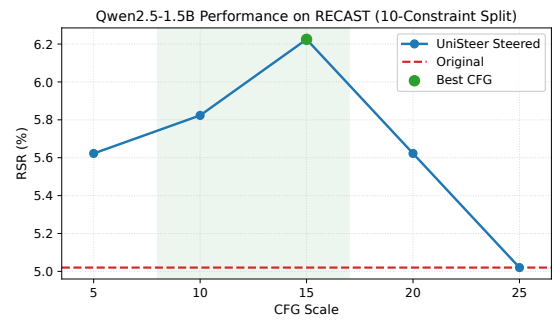
(a) RECAST-5 sweep for Llama-3.2-1B.



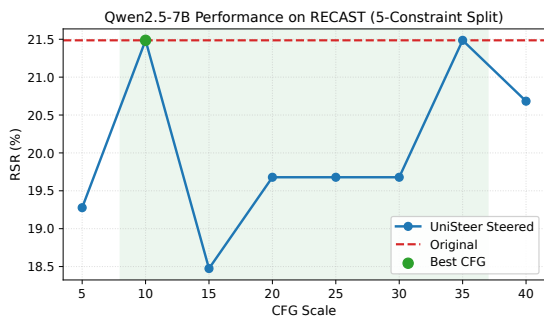
(b) RECAST-10 sweep for Llama-3.2-1B.



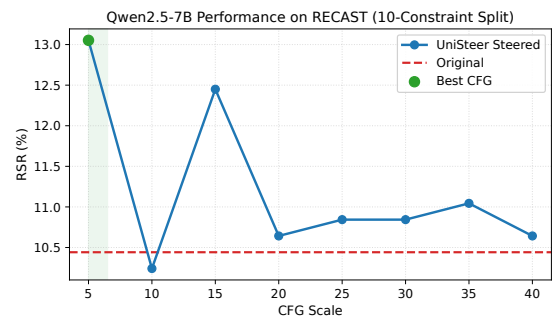
(c) RECAST-5 sweep for Qwen2.5-1.5B.



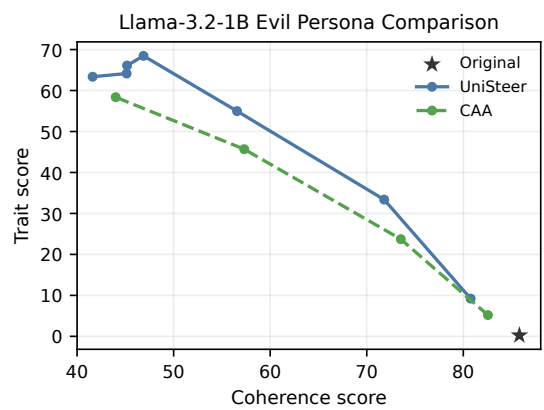
(d) RECAST-10 sweep for Qwen2.5-1.5B.



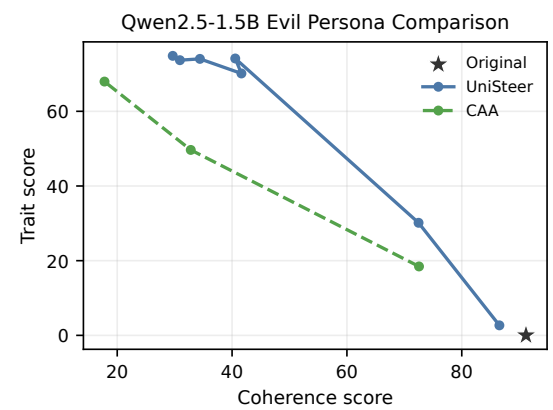
(e) RECAST-5 sweep for Qwen2.5-7B.



(f) RECAST-10 sweep for Qwen2.5-7B.



(g) Llama-3.2-1B (Trait-coherence).



(h) Qwen2.5-1.5B (Trait-coherence).

Figure 4: Hyperparameter sweeps on RECAST (top three rows) and Trait-coherence trade-off on the Persona evil trait (bottom row).